The Astrophysical Journal, 658:1372–1379, 2007 April 1

ARE MORETON WAVES CORONAL PHENOMENA?

K. S. Balasubramaniam, A. A. Pevtsov, and D. F. Neidig[1]
National Solar Observatory, Sunspot, NM 88349; bala@nso.edu, apevtsov@nso.edu, neidig@nso.edu
Received 2006 June 5; accepted 2006 December 15

ABSTRACT

We report on permeability characteristics of the upper solar atmosphere due to the progression of a Moreton wave. An exceptional Moreton wave is tracked to cover most of the Sun, following an unusually large solar X-ray flare observed on 2003 October 29. Using Hα intensity and Doppler measurements, the Moreton wave is tracked for as long as 12 minutes. Moving outward, the wave circumnavigates strong-field active regions. The wave sweeps through solar magnetic neutral lines, disrupting material from filament and filament channels, thereby accentuating the visibility of the wave. We establish that the requirement for the visibility of a Moreton wave is the necessary presence of higher density material in the layers of the corona, besides reaffirming that Moreton waves are observed only when the speed of the disturbance exceeds Mach 2. We suggest that the cause can be a removal of significant amount of material from the solar upper atmosphere due to a coronal mass ejection.

Subject headings: stars: activity — stars: coronae — stars: chromospheres — stars: magnetic fields — Sun: activity — Sun: chromosphere — Sun: corona — Sun: coronal mass ejections (CMEs) — Sun: filaments — Sun: flares — Sun: magnetic fields — waves

1. INTRODUCTION

Moreton waves have been recognized as solar chromospheric surface waves observed immediately following large solar flares (Moreton 1960; Athay & Moreton 1961; Dodson & Hedeman 1968; Smith & Harvey 1971; Narukage et al. 2004; Okamoto et al. 2004). As identified in the hydrogen Hα (H I 6562 Å) spectral line and its off-band Dopplergrams, a typical Moreton wave appears as a propagating dark/white front (corresponding to up-down motion). In some cases, Moreton waves are identified with erupted filaments, and in other cases they have been identified with filament oscillations and/or with the "flickering" of distant filaments when the wave passes by them. The flickering was attributed to the up-down oscillations of filaments that move material in and out of the observed Hα bandpass. The Moreton waves usually last for 3–6 minutes, extending over a limited sector angle [60″–120″; arc extent of $\sim(130–220) \times 10^3$ km perpendicular to the propagation] away from the flare source at 500–2000 km s^{-1}. It is important to emphasize that, to date, all observed Moreton waves have been limited to small sector angles, as mentioned above.

The earliest significant effort to model the propagation of Moreton waves was by Uchida (1968). In his model, a solar flare initiates a coronal shock disturbance that propagates as a hydromagnetic fast-mode wave whose front has a circular intersection line with the upper chromosphere. The chromospheric (Moreton) wave is then treated as an acoustic wave due to the refraction of the coronal wave at this intersection. Since Moreton waves were observed on only one side of the flare, Uchida suggested that this asymmetry was due to a limited-directivity explosion of the flare, or to the assumption of an arbitrary magnetic wall in the nonobserved side. Additional models treated Moreton wave phenomena in a framework of shock and blast waves (e.g., Vršnak et al. 2002; Hudson et al. 2003; Chen et al. 2005). Despite differences in physical interpretation, most models consider explosive release of energy (a flare due to heating and expansion) as a trigger for the Moreton wave. Extending this argument, if one considers two or more separate but near-simultaneous (e.g., sympathetic) flares, we should expect two or more different Moreton waves originating from different flare sources. Although such flares do occur, there are no reports of multiple Moreton waves originating from distinctly different flare sources. This calls into question explosive flare events as a cause of the Moreton waves. Some recent studies (e.g., Cliver et al. 1999) suggest that Moreton waves may originate from fast coronal mass ejections. (CMEs)

During a prolific period of solar activity in 2003 October–November, major solar storms from solar flares and CMEs resulted in intense space weather and related geomagnetic disturbances (Gopalswamy et al. 2005). One such event, the X10 flare on 2003 October 29 (20:38 UT), resulted in an unprecedented Moreton wave with spatial and temporal properties that have previously never been observed. In a study of coronal waves related to explosive events, Warmuth et al. (2005) mention that this event is accompanied by coronal waves seen in Hα, *SOHO* EIT, soft X-rays, and He I measurements, and that the Moreton wave for this event has both northward and southward components. Recently, Liu et al. (2006) have reported on the relationship between remote brightenings (also known as sequential chromospheric brightenings [SCBs]; e.g., see Balasubramaniam et al. 2005) related to this event and the accompanying CME, flare, and Moreton waves. Therein, Liu et al. speculate on the possible magnetic connections between the remote brightenings and the flaring region. They find that the timings of the remote brightenings coincide with neither Moreton waves nor type II bursts. Hence, according to Liu et al., neither of these two mechanisms (Moreton waves and type II bursts) can be the trigger of the remote brightenings. The essential aim of the work of Liu et al. (2006) in studying Moreton waves is to prove that Moreton waves do not trigger the remote brightenings.

In contrast, the present work describes the propagation characteristics of this exceptional Moreton wave and uses arguments from spectral line formation and wave speeds to affirm its presence as a coronal rather than chromospheric phenomena. We only mention SCBs in passing.

In the following sections we describe the observational data sources, present our analysis, and investigate the characteristics of the chromosphere. We discuss the vertical location of the Moreton

[1] NSO Emeritus Astronomer.

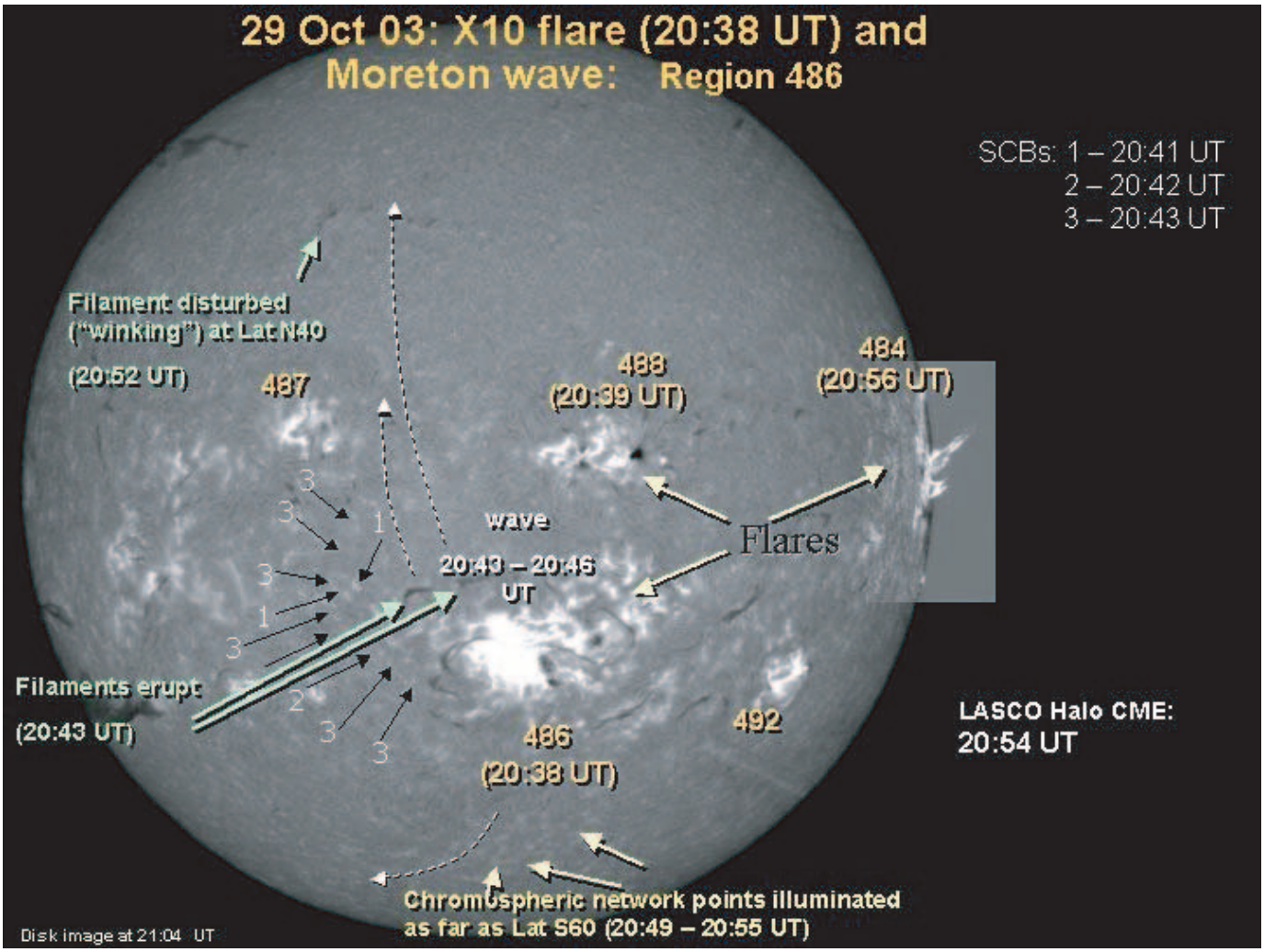

FIG. 1.—Full-disk ISOON Hα image on 2003 October 29. The positions of the flare, the SCBs, and the waves from Hα, as well as the Hα running-difference images, are noted.

wave in the outer atmosphere, and provide arguments for coronal location of Moreton wave. We note that some preliminary results of this work were presented as oral paper at an AAS meeting (Neidig 2004).

2. DATA SOURCES

The observations were recorded on 2003 October 29.

The ground-based USAF/Optical Solar Patrol Network (O-SPAN, formerly known as ISOON; Neidig et al. 1998) telescope recorded the entire event. Solar full-disk images were acquired at Hα line center (at 6562.8 Å, bandpass of 0.1 Å) and its spectral line wings at $\pm$0.4 Å, with a cadence of 1 minute. The innovative design of O-SPAN allows the acquisition of high-quality, Hα, full-disk images with unprecedented clarity. A pair of tunable Fabry-Perot etalons in a telecentric optical configuration and a photometric quality CCD camera is central to O-SPAN's superior performance. These produce a high-throughput, short-exposure (20 ms) image acquisition system, with high spectral purity. Doppler images (interpreted as line-of-sight velocity) were reconstructed from the difference of wing images, at Hα $\pm$ 0.4 Å. The Hα blue and red images are acquired sequentially within a time of 3 s. This $\approx$3 s time difference in the acquisition of the blue and red images causes negligible impact on the wave measurements that are a minute apart. The spatial pixel projected on the Sun was 1.1 arcsec^2 ($\sim$798 square km).

In addition to O-SPAN's Hα data, we use the well-established solar full-disk photospheric magnetograms (pixel size = 2″) acquired by the Michelson Doppler Imager (MDI; Scherrer et al. 1995) on board the *Solar and Heliospheric Observatory* (*SOHO*). To develop a larger perspective of the event, we used additional observations from two other *SOHO* instruments: 195 Å images from the *SOHO* Extreme Ultraviolet Imaging Telescope (EIT; Delaboudiniere et al. 1995). The EIT images have an approximate cadence of 12 minutes. We use coronal images from the online Large Angle Spectrometric Coronagraph (LASCO; Brueckner et al. 1995) Catalog (Yashiro et al. 2004) to identify CMEs associated with this event. The LASCO images span a field of view of 2–30 $R_\odot$ and have cadences of 30 minutes in the inner field of view (2–6 $R_\odot$) and 60 minutes in the outer field of view (6–30 $R_\odot$).

3. SPATIAL CHARACTERISTICS OF THE MORETON WAVE

First, we describe the spatial characteristics of the waves observed in Hα line core images and Dopplergrams derived from the wing (Hα $\pm$ 0.4 Å) images.

3.1. Hα *Line Core Images*

Figure 1 summarizes the flare and the direction of propagation of the wave in this remarkable event as observed in the core of Hα line. The strong Hα flare (*GOES* X10 in X-ray) is first seen at

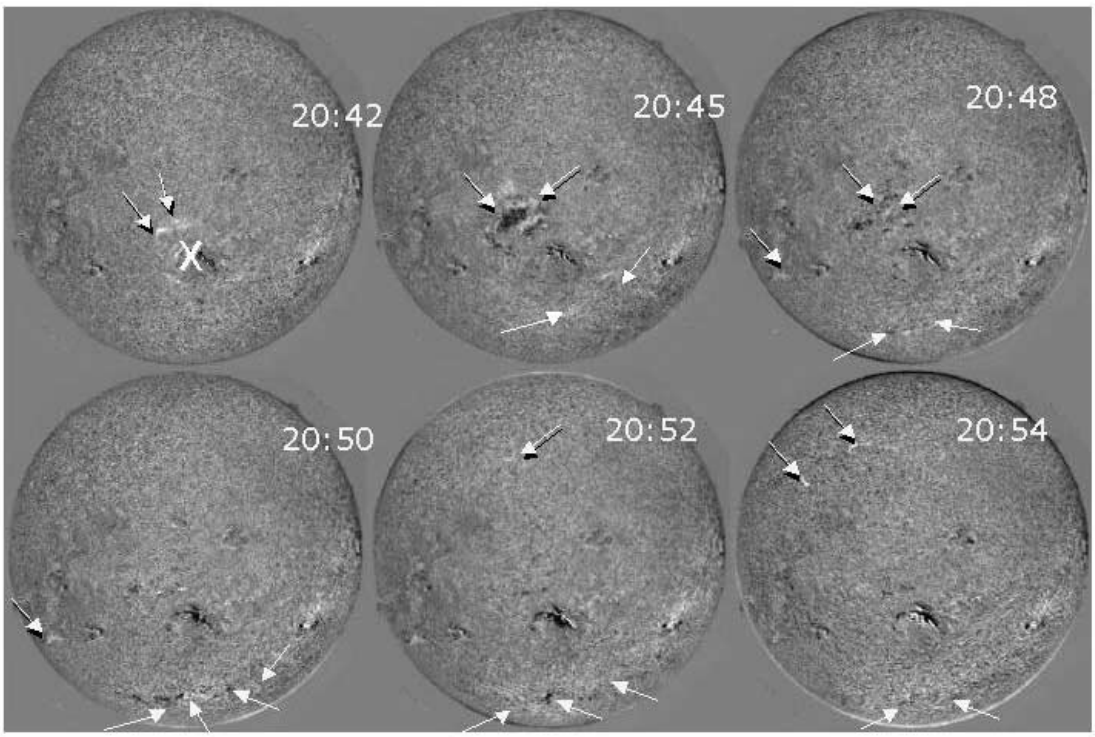

FIG. 2.—Sequence of Dopplergrams depicts the propagation of Moreton waves at different times. Point X in the top left panel indicates the position of the flare. The arrows at 20:42 point to the position at which the filament begins to disperse and disappear. The three ridges formed during the initial part of the Moreton wave are seen in the panel at 20:52. Arrows point to the progression of the Moreton wave at different times.

20:38 UT in active region (AR) 10486, in the southern hemisphere. A near simultaneous flare is seen in the neighboring AR 10488 at 20:39 UT, in the northern hemisphere. Following these two flares, a series of SCBs light up the network points (labeled 1, 2, and 3 in Fig. 1), between 20:41 and 20:43 UT. According to Balasubramaniam et al. (2005), SCBs are progression signatures of a coronal mass ejection (CME) that are visible in the chromosphere, at footpoints of magnetic field lines that extend into the corona.

An expanding Moreton wave is seen in Hα line core images (Fig. 1) and is confirmed in animation movies of Hα running time-differenced images (difference of two successive images, separated by 1 minute), about 2 minutes following the SCBs. This wave starts in vicinity of AR 10486 at about 20:43 and initially is detected propagating in a northeast direction (toward AR 10487) with an approximate speed of 1100–1200 km s^{-1}. The wave is identified as an intensity enhancement. The speed was inferred by measuring the positional displacement of the wave front in successive images in the plane of the sky. As the wave front crosses the two small filaments (overlying a photospheric magnetic neutral line), its contrast increases. Examining the Hα line core images individually, we find that segments of both filaments initially become diffuse and broad (20:42–20:43), and then completely disappear between 20:44 and 20:45. Segments of the filament reappear between 20:46 and 20:50, and the filament reforms completely between 20:53 and 20:57, almost returning to its original geometry. This sequence of observations indicates that material associated with several fragments of filaments probably erupted due to the passing wave, followed by their quick reformation. We note that the observations show no indication that the entire filament erupted, and this was partial eruption. The wave then appears to avoid AR 10487 and follows a northerly direction at 20:46 UT, through a quiet-Sun region between AR 10487 and AR 10488. At that point, the wave gradually fades as it appears to propagate further northward. At 20:52 UT, another filament, situated northeast of AR 10487, at latitude N40°, is disturbed. A small segment of this filament disappears, and the contrast in the Doppler images increases, indicating that the Moreton wave continues its journey across solar surface.

A southward-propagating component of the wave is also seen, although its contrast is poorer and less readily identifiable as its northern branch. We note that in this southern portion of the Sun, the region is relatively free of activity and magnetic fields, as identified from Hα intensity images and MDI magnetograms. The wave is somewhat enhanced at first, far to the south of AR 10486, near the location of a magnetic neutral line, and is seen as a series of chromospheric network points progressively illuminated between 20:49 and 20:55 UT (see Fig. 1, *bottom*). The broken-arrow line indicates the direction of sequential illumination. The propagation is seen as far as lattitude S60°. The total duration of the wave in both hemispheres is about 12 minutes, which is exceptionally long in comparison to previously observed Moreton wave phenomena (3–6 minutes). Although there is no observational evidence for the wave propagating northwest from AR 10486, a flare was observed in AR 10484 at the west limb. The timing of the flare indicates that this eruption coincides with the time of the wave reached this active region. However, this flare could also be the result of a global connectivity in solar corona, and could have been triggered by a coronal mass ejection (CME).

3.2. Hα *Dopplergrams*

Dopplergrams acquired in the wing of the Hα spectral line provide firm evidence for the presence of Moreton waves with amplitudes large enough to produce vertical displacements in the solar atmosphere. Using Hα Dopplergrams (temporal cadence of 1 minute) between 20:42 and 20:54 UT (Fig. 2), we find that the first visibility of Moreton wave appears about the same time the filaments are partially disrupted (see Figs. 1 and 2) at 20:43 UT.

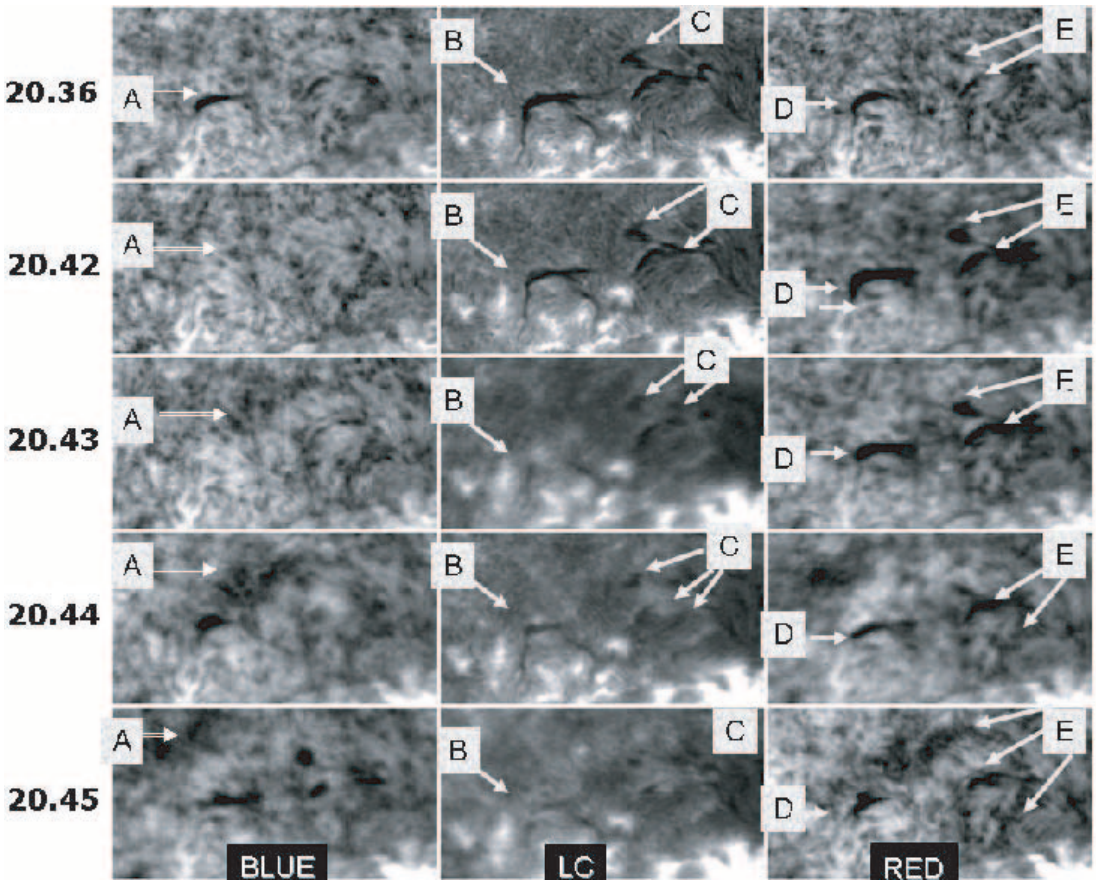

FIG. 3.—Individual spectrograms at the line center and the blue and red wings of the spectral line. The field of view is 330″ × 180″. The time sequences are 2 minutes before the flare and during the Moreton wave progression between 20:42 and 20:45 UT, respectively. Note the two sets of "helmet"-like loops and their disruption with the passage of the Moreton wave.

In Figure 2 a sequence of Dopplergrams depicts the propagation of Moreton waves at different times. Point X in the top left panel indicates the position of the flare. The arrows at 20:42 point to the position at which the filament begins to disperse and disappear. The three ridges formed during the initial part of the Moreton wave are seen in the panel at 20:52. Arrows point to the progression of the Moreton wave at different times. The filaments are partially disrupted in the direction of the Moreton wave propagation. This partial disruption and dispersion is similar to that seen in the line core images. A recent report on the statistics of relating Moreton waves to erupting filaments (Narukage et al. 2004) demonstrates convincingly that the direction of erupted filament is in the same as the propagated Moreton wave. The Moreton wave for this event as seen in Doppler images coincides with the propagating wave as seen in Hα line core images. In the vicinity of the erupted filaments the Moreton wave as seen in Doppler images appears far more complex, having at least three down-up wave trains rather than one down-up half-wave of typical Moreton waves. It is a propagating wave train encompassing three full spatial wavelengths (see Fig. 2).

4. DOPPLER MEASURE OF THE MORETON WAVE SHALLOWNESS

Using this information, we estimate the penetration depth of Moreton wave. From Figure 2, the observed spatial span of the waves, from the leading edge to the trailing edge of the three wave trains, is about 200,000 km, which is comparable to the dimension perpendicular to the direction of propagation in these two-dimensional images. The wavelength varies from the leading edge to trailing edge, as well as from side to side, and attains a maximum value of about 88,000 km (distance between ridges). As shown in the Figure 2 at 20:45 UT, the imprint of the wave shows an elliptical structure with the long axis perpendicular to the direction of propagation; this complex structure suggests both a strongly dispersive nature of the wave and a vertical modulation that is perhaps governed by the overlying coronal disturbance. From successive images, the wave's speed is measured to be 1100–1200 km s^{-1}. Thus, with a wavelength of 88,000 km, a wave period is estimated to be 80 s. The brightness the wave structure in Hα Doppler images is used in conjunction with a spectral line profile model to estimate the line shift. The result is 0.57 Å, which corresponds to a vertical velocity amplitude of 2.6 km s^{-1}. Fitting the latter to a sinusoidal displacement variation yields an implied displacement of 66 km. This estimate contradicts that the Moreton wave appears in both in the line core and wings of Hα. We discuss this inconsistency in § 9.

5. DISTURBED FILAMENTS AND FILAMENT CHANNELS

To understand the nature of the partial filament disruption for the two small filament structures northwest of AR 10486 (Fig. 2, *long double arrows at 20:42 UT*), we present a time-evolution sequence of original resolution individual spectrograms in theline center and the blue and red wings of the spectral line (see Fig. 3). The time sequences are 2 minutes before the flare and during the Moreton wave progression between 20:42 and 20:45 UT, respectively. The field of view (Fig. 3) shown on each panel is 330″ × 180″. We bring to the readers attention the two sets of

"helmet"-like loops. Segment A is present in all three filter pass-bands of the filament appears well defined at 20:36 UT. As seen as a time-evolution in the blue wing, segment A appears to diminish, move, spread, and disperse at times 20:43 and 20:44 UT. Note that a small thickened segment of A quickly reappears, after briefly being absent. The dispersion and spreading of this segment of the filament is clear and is the part of the Doppler ridge reconstructed in Figure 2. Let us examine segment B (Fig. 3) of the same filament in the line core images (marked B) and red-wing images (marked D). The core images show that the filament thins out between 20:36 and 20:42, while segment D in the red wing thickens. In successive temporal images of the line center, and the filament (B) partially vanishes, while in the red wing, it first thickens (at 20:42), then thins out and considerably disperses over a larger area (at 20:45). Similarly, examining elements C and E in the line center and the blue and red wings, we note that the filament not only changes its shape and position, but also disperses into a larger area. We bring the reader's attention to the red panel at 20:45 and the spreading of the filament indicated by E. The spreading of the shredded fragments of the filament marked E is also present (although fainter) in spatial positions corresponding to the blue and line center images. A rapid-sequence animation of these images extended over a larger time range clearly demonstrates that the filaments are being partially disrupted and the resultant material is being disbursed. In all these cases, one can see shreds of filament disappearing and reappearing, pointing out the possibility of quick disruption and reformation of the cooling material in magnetically stable pockets.

Taking into account the propagation speeds of the Moreton wave, we conclude that the filament oscillation (winking, as seen Doppler images) at latitude N40° coincides with the arrival time of the Moreton wave at the filament location. This supports the impression, from high-speed animation of the Doppler images, that the filament winking is a part of the underlying disturbance. This inference is further supported by the fact that the Doppler images taken at 20:52 UT (Fig. 2) show a faint pattern of white/dark ridges, similar in appearance to a pattern observed earlier at 20:45 UT. We note that this conclusion contradicts Liu et al. (2006), who suggested that disturbance of these two filaments is unrelated to Moreton waves. We recall the works of Narukage et al. (2004), who also note that disturbed or erupted filaments are significantly related to Moreton waves in both timing and direction.

Similarly, the southward-propagating component of the Moreton waves is visually enhanced after crossing the magnetic neutral line (Fig. 4, *blue line*) in the southern hemisphere, between 20:49 and 20:55 UT. Since filament channels are resident above photospheric neutral lines, and since filaments are suspended above the mean chromosphere, by induction we can assert that the filament-like material in filament channels is swept by the Moreton wave, hence enhancing the visibility of the wave in lower altitudes. We must note that the southward-propagating wave is too faint. Two reasons can contribute to its faintness near the limb: first, the predominant radial motion of the wave will contribute only a weak Doppler signal near the limb; second, the limb darkening weakens the signal, and hence we are unable to make meaningful measurements of its amplitude. The temporal extent of the Moreton wave in both hemispheres is coincident with the wave identified in the Hα line-center image and also lasts about 12 minutes in total.

6. THE MORETON WAVE AND CORONAL COUNTERPARTS

The *SOHO* EIT 195 Å images, at and prior to 20:33 UT, show the presence of a transequatorial loop (TL; Pevtsov 2000) system that exists between AR 486 (S17E4) and AR 488 (N8W4). In the following *SOHO* EIT 195 Å image (at 20:48 UT) the TL is fainter and has moved (and is absent later on), possibly having erupted in conjunction with the flare. Animation sequences of the EIT temporal difference images (not shown) indeed affirm an erupted TL system. On the other hand, from the animation sequence of the EIT or time-differenced EIT images we do not see convincing indications of an EIT wave. It is possible either that the EIT wave is either entirely absent or that an EIT wave does not show up due to insufficient cadence of the EIT data (we note, however, that Warmuth et al. (2005) reported an EIT wave front north of the erupting CME for this event). We also note that Liu et al. (2006) do not find sufficient evidence for the presence of EIT waves. As a note of interest, the research literature has examples of Moreton and EIT waves that are traced to the same disturbing source and have the same propagation characteristics for the short duration for which the Moreton waves are seen. For this exceptional event, there is no such parallel.

The *SOHO* LASCO catalog (Yashiro et al. 2004) lists a halo CME detected at 2003 October 29, 20:54 UT with a linear speed of about 2090 km s^{-1}, projected in the plane of the sky. The significant difference in speeds of the CME (outer corona and heliosphere), relative to the Moreton wave ($\sim$1200 km s^{-1}), perhaps reflects the differences between the densities in the two regions, and perhaps shows different aspects of the same phenomena. It is also possible that the radial expansion speed of CMEs as seen by LASCO is somewhat different from the lateral expansion of the CME, closer to the solar surface. Similar to Liu at al. (2006), we have also independently used the backward extrapolation, using the timing, speed, and height of the CME to infer that the CME must have be triggered at about 20:42, which is coincident with the timing of the flare. Hence the flare and the CME appear to be triggered by conditions at the AR 10486.

More importantly, the detection of a CME bolsters the fact that the Moreton wave is produced in connection with an eruptive coronal event. Unlike Liu et al. (2006), we do not discuss the events of coronal dimming, which are measurements about $\approx$3 hr after the flare, much beyond the scope of the temporal extent of the Moreton wave.

7. THE MORETON WAVE AND THE UNDERLYING MAGNETIC FIELD

Using the locus of an expanding and outwardly propagating Moreton wave, we have contoured the outline of the Moreton wave at each instance between 20:43 and 20:55 UT. The successive gray-scaled contours, from light to dark, sequentially trace the evolution of the Moreton wave as an integrated snapshot. The blue lines in Figure 4 outline the position of the photospheric magnetic neutral lines near filaments and filament channels. The position of the magnetic neutral line was determined from the *SOHO* MDI magnetograms.

From this integrated image we notice that the Moreton wave first appears at neutral lines that have filament material (filaments or filament channels). It appears that the filament material is dispersed with the onward propagation of the wave. We also observe that the Moreton wave avoids strong magnetic fields (>several hundred Gauss; active-region fields), while it plow through weak magnetic fields (100 Gauss or less) and magnetic neutral lines. We see here an important distinction between this Moreton wave and waves that have been previously studied in EIT images (Moses et al. 1997; Thompson et al. 1998, 1999). EIT waves propagate inhomogeneously and avoid strong magnetic fields (Thompson et al. 1999). So do Moreton waves. In contrast, EIT waves avoid neutral lines, stop near coronal holes (magnetic boundaries between open and closed field lines; Thompson et al. 1999), and

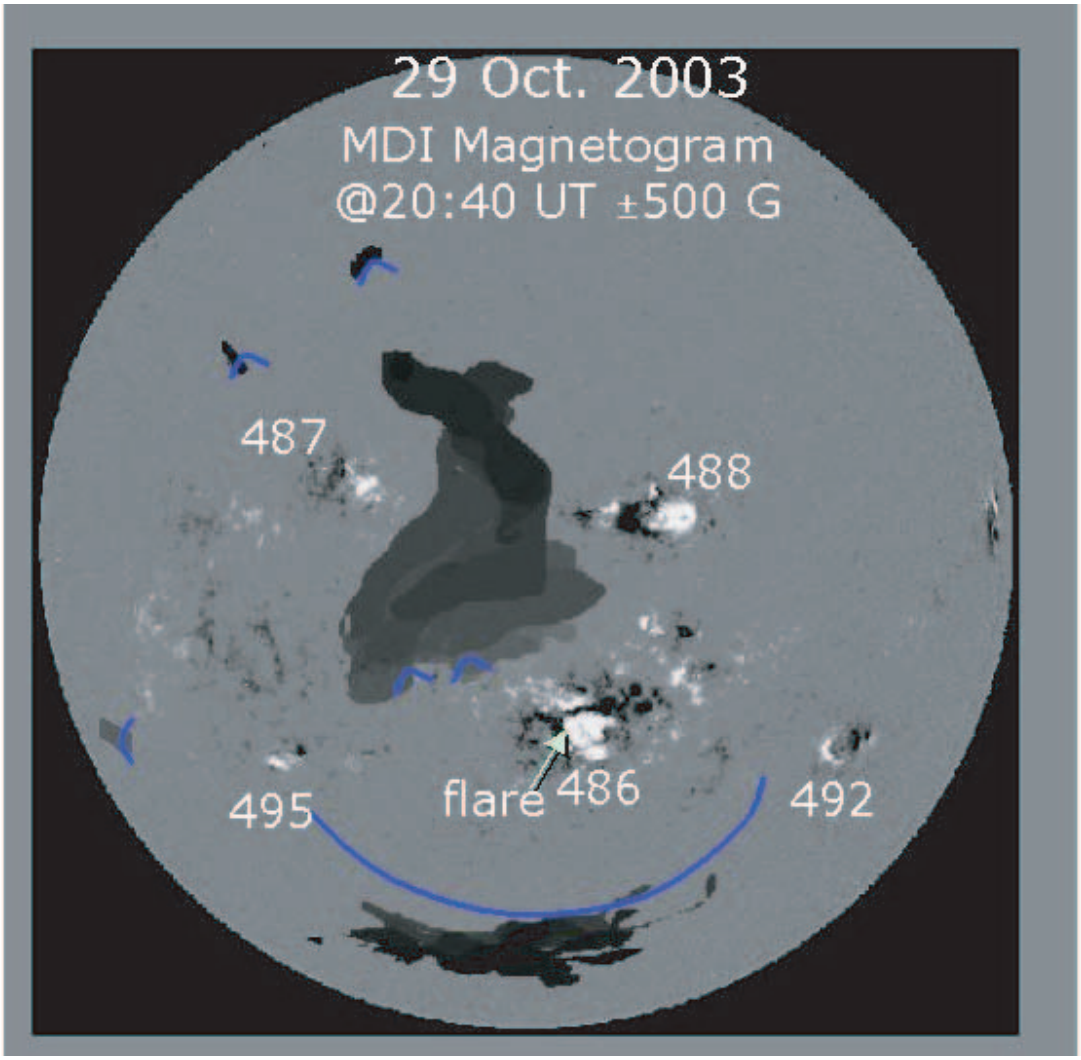

FIG. 4.—*SOHO* MDI magnetogram taken during a time of exceptional activity, 2003 October 29. Contours of the positions of Moreton wave at different times are superposed. Each gray scale, from the lightest to the darkest, traces the positions of the Moreton waves at different times. Blue lines indicate the position of magnetic neutral lines.

stop near magnetic separatrices between active regions (Delanée & Aulanier 1999). The Moreton waves shown here are first observed when they cross neutral lines or filaments.

Liu et al. (2006) also noted that the northern component first propagated in the northeast direction and then changed its direction northward, possibly because it encountered a coronal hole. An overlay of the magnetogram on top of the expanding outer contours of the Moreton wave demonstrates that beyond the coronal hole lies stronger field magnetic regions, which could be an additional reason why the wave direction is diverted.

8. SPEED OF MORETON WAVES AND VISIBILITY

Warmuth et al. (2001) argue that Moreton waves can be seen only when the Mach number, M, exceeds a value of 2 ($M > 2$). The speed of the wave is

$$v_f = M\nu_{\rm ms},$$

where $\nu_{\rm ms}$ is the magnetosonic speed. Following Warmuth et al. (2001), we assume $\nu_{\rm ms} = 300$ km s^{-1}, and taking the measured speed of the Moreton wave nearest to the first filament eruption to be $\sim$1200 km s^{-1}, we find that this wave has a Mach number of 4. Despite the speed being larger than previously established, the visibility of the Moreton wave is enhanced only after it encounters higher density filament material and disperses the filament material, or when it crosses areas of enhanced density, such as filament channels. That is, Moreton waves do not appear automatically when the speed exceeds a certain critical value. An additional condition for the visibility of these waves, at least in this case, is the presence of enhanced density material (filaments) that can be recognized by observations.

9. DISCUSSION AND CONCLUSIONS

We have described an exceptional sequence of events starting from the X10 flare of 2003 October 29, and the trail of disturbances that include SCBs, filament eruptions, a propagating wave in the Hα line core, a Moreton wave in Hα Doppler images, multiple flares in distant active regions, and disturbing of distant filaments. These high spectral resolution imaging observations have shown the unusual lifetime of the wave, which lasts as long as 12 minutes and encompasses almost the whole Sun. This contrasts with historical descriptions of Moreton waves from Hα Doppler images lasting only 2–6 minutes. Of particular interest is that the wave avoids strong magnetic field sunspot regions,

while plowing across neutral lines, partially carrying away filament material from filaments and filament channels. Moreton waves in the past have been known to show small segmented arcs from the site of the flare. Due to the exceptional nature of the wave, we are able to observe a larger angular extent, continuity, and expansion of the wave.

From these measurements we had derived that the Hα Moreton wave affects a thin ($\sim$66 km) portion of the atmosphere. This small thickness contradicts the fact that we see Moreton waves both in the line center and the wings, whose heights of formation are approximately separated over a range of $\approx$500 km. To resolve this contradiction, we propose that in the presence of filament material the contribution functions for Hα changes in such a way that we see coronal material contributing to the chromospheric line.

Radiative transfer calculations of an average chromosphere result in a height of formation of the core of the Hα line ($\tau_{500} = 1$) between 1600 and 3000 km (White & Wilson 1966). New and detailed radiative transfer calculations by H. Uitenbroek (2006, private communication) show that contribution function of the core of the Hα line ($\tau_{500} = 1$) is formed at a height centered about 1900 km, while the wings of the H$\alpha \pm 0.4$ Å ($\tau_{500} = 1$) are formed centered about 1000 km. In the past, radiative transfer arguments were used to place the Moreton wave in the mid- to upper chromosphere. We believe that this approach can be misleading.

Limb observations of filaments show that Hα filaments exist at a height >several 10,000 km above the average chromosphere, well above the quiet chromosphere. Radiative transfer inversions of the observed heights of formation of filaments measured by Schmieder et al. (2004) suggest that the filaments are present at heights of $(50–120) \times 10^3$ km above the limb, and are essentially coronal structures that show up in the Hα absorption simply due to presence of cooler hydrogen gas. Hence, there appears to be a significant jump in contribution function of the layers that contribute to the Doppler signal from the quiet-Sun chromospheric elements to those (coronal) structures where filaments are present. This change in contribution function in the presence of cool Hα material on the corona perhaps causes the appearance of coronal phenomena in the chromospheric spectral line. On the other hand, the contribution of coronal material could result in only a slight asymmetry in the Hα line profile. Interpreting this slight asymmetry in the framework of Doppler shifts can underestimate the line-of-sight velocities significantly. The atmospheric segment that participates in the disturbance is significantly thicker than 66 km (even though each individual chromospheric layer is displaced only by a smaller amount). In other words, the spectral line could have two components, a larger contribution due to the chromosphere and a small coronal contribution due to filament material. Even if the coronal component exhibits high Doppler shifts, its weak contribution when convolved with the main chromospheric component displays small resultant Doppler shifts. This perhaps explains the *apparent* shallowness (66 km) measure of the Moreton wave, which was derived using the vertical displacement of the entire Hα spectral line, while we know that the filament body itself might extend several hundred kilometers in extent. A further understanding of this process can be addressed by two-component or multicomponent radiative transfer calculations that can separate out chromospheric and coronal contributions.

We suggest that Moreton waves are not always chromospheric imprints of coronal waves as pointed out in previous studies (Gilbert et al. 2004), but have a significant coronal component. For this event, the fact that Moreton waves are enhanced at the location of magnetic neural lines/filament channels further supports this idea. We suggest that Moreton waves also propagate in the corona at heights of a few times 10^4–10^6 km. (This height range comes from the approximate height at which where filaments are formed.) This implies that Moreton waves also propagate in quiet-Sun areas, where filament channels do not exist. The presence of cool material in filament channels changes the contribution function and the wave appears in the chromospheric spectral line. The Moreton wave becomes more pronounced when crossing filament channels and neutral lines. The event observed is unique in both data quality and coverage to follow partial filament disruptions, winking of filaments, and the wave crossing neutral lines. The presence of cold coronal material in filament channels (above neutral lines) changes the contribution function of Hα, which makes Moreton waves appear in the chromospheric lines. We use filament eruption as indicators of the disruption of the cold material and passing of the Moreton wave. The filaments are partially disrupted in the direction of the Moreton wave propagation (also see Narukage et al. 2004). This scenario may appear to be at odds with some observations of the past that show Moreton waves may propagate over the quiet-Sun. However, past observations of quiet-Sun waves did not compare location of Moreton wave enhancements and filament channels. In many cases, filament channels may not be clearly identifiable in "traditional" Hα images. Hence, additional studies are needed to qualify these observations.

As an additional argument, the speed of the Moreton wave, $\sim$1200 km s^{-1}, well exceeds the sound speed (8–10 km s^{-1}) of the chromosphere by almost 2 orders of magnitude. If the Moreton wave were to propagate inside the chromosphere, it would be quickly dissipated, and the chromosphere would not be able to sustain a Moreton wave for long periods of time. This argument further supports the deduction that Moreton wave propagates above the chromosphere, and in the corona, which was a motivation for Uchida (1968) to consider the coronal origin of the wave.

We agree with Liu et al. (2006) that Moreton waves are not the trigger of SCBs (or remote brightenings). SCBs precede Moreton waves by as much as 2 minutes. This bolsters the proposition that SCBs and Moreton waves are perhaps formed at different layers in the solar atmosphere. A coronal rather than chromospheric origin of the Moreton wave lends further credibility to the idea that SCBs and Moreton waves are a part of a global eruptive mechanism that manifests itself in different layers.

Several additional questions need to be addressed in making detailed models to understand the trigger source of this exceptional event or similar events in the future. We observe multiple flares from different active regions (see Fig. 1) that are nearly simultaneous; however, there is just a single Moreton wave. Why do we see only a single Moreton wave despite multiple sympathetic flares? It has not been conclusively proven that flares are (or are not) the definite trigger of Moreton waves, but their closeness in time is rather suggestive. A counterargument to triggering of Moreton waves is that if one were to consider (an imaginary situation) when there are two (or more) spatially separate but near-simultaneous, sympathetic flares, then one should expect two (or more) distinct set Moreton waves. As previous studies of Moreton waves have suggested that this is a disturbance propagating the chromosphere, in turn, we argue that this is purely a coronal phenomena. There is better evidence for Moreton waves having a coronal origin, as flares have a significant chromospheric origin.

Furthermore, the timing and speed of the Moreton wave front disagrees with the conjecture that the flare has to be the origin of the wave. For a moment, let us first assume that the flare kernel (at 20:38 UT) was the source of the Moreton wave. Assuming

that the Moreton wave was initiated with a linear speed of $\sim$1200 km s^{-1} (as observed), 8 minutes later (at 20:45 UT) the wave should have traversed a distance of 576,000 km. However, using the data shown on the top middle panel of Figure 2, we see that the wave has really traveled only a distance of about 360,000 km. Although we cannot rule out decelerations (earlier), we note that the wave maintains a fairly constant speed. Hence the wave was possibly triggered by a mechanism that occurred after the flare, e.g., a CME lift-off, or it possibly has an extended origin situated outside (eastward) of AR 10486—which again points to a CME. The extent of the wave attests to the trigger being a global extended coronal source rather than a compact source (flare), perhaps the overlying CME. Once can envision the following sequence of events: A ballooning CME removes a significant volume of coronal plasma and triggers the Moreton wave in the corona. As the wave encounters areas with significant cool coronal material, the material is swept resulting in the enhanced Doppler visibility, as it appears in the "chromospheric" Hα line measurements.

The following caveats are in order. The enhanced wave-front signatures after passing the filament can only be partially attributed to fragments of the filament dispersing. It should be noted that not the entire filament was disrupted. Since filament oscillations and winking of filaments have also been observed during the passage of Moreton waves, the disruption of filaments does not exclusively identify a Moreton wave. Partial disruption of filaments and the resultant dispersal of material is just one mechanism that identifies the waves.

The above scenario is supported by observations of a single unique event, and strengthened by previous observations of filament disruption in the direction of the Moreton wave. However, further investigations with a larger number of events are necessary to establish our findings. Furthermore, our inference that Moreton waves exhibit enhanced wave-front signature due to the presence of enhanced filamentary material is not the only explanation. Again, further studies are necessary to distinguish between this and other models of Moreton wave propagation.

The National Solar Observatory is operated by the Association of Universities Research in Astronomy (AURA), Inc., for the National Science Foundation. The Air Force Research Laboratory, Space Vehicles Directorate, at NSO, Sunspot, NM, operates O-SPAN. *SOHO* is a project of international cooperation between ESA and NASA. The LASCO CME catalog is generated and maintained by NASA and The Catholic University of America in cooperation with the Naval Research Laboratory.

We thank Han Uitenbroek for a providing us with an example of detailed calculation of the heights of formation of the Hα line, in quiet-Sun, hydrostatic atmospheres. Critical comments by an anonymous referee have helped improve the manuscript.

REFERENCES

Athay, R. G., & Moreton, G. E. 1961, ApJ, 133, 935
Balasubramaniam, K. S., Pevtsov, A. A., Neidig, D. F., Cliver, E. W., Thompson, B. J., Young, C. A., Martin, S. F., & Kiplinger, A. 2005, ApJ, 630, 1160
Brueckner, G. E., et al. 1995, Sol. Phys. 162, 357
Chen, P. F., Fang, C., & Shibata, K. 2005, ApJ, 622, 1202
Cliver, E., Webb, D. F., & Howard, R. A. 1991, Sol. Phys., 187, 89
Delaboudiniere, J.-P., et al. 1995, Sol. Phys., 162, 291
Delannée, C., & Aulanier, G. 1999, Sol. Phys., 190, 107
Dodson, H. W., & Hedeman, E. R. 1968, Sol. Phys. 4, 229
Gilbert, H. R., Holzer, T. E., Thompson, B. J., & Burkepile, J. T. 2004, ApJ, 607, 540
Gopalswamy, N., Yashiro, S., Liu, Y., Michalek, G., Vourlidas, A., Kaiser, M. L., & Howard, R. A. 2005, J. Geophys. Res. 110, A09S15
Hudson, H. S., Khan, J. I., Lemen, J. R., Nitta, N. V., & Uchida, Y. 2003, Sol. Phys., 212, 121
Liu, C., Lee, J., Deng, N., Gary, D. E., & Wang, H. 2006, ApJ, 642, 1205
Moreton, G. E. 1960, AJ, 65, 494
Moses, D., et al. 1997, Sol. Phys., 175, 571
Narukage, N., et al. 2004, in Proc. IAU Symp. 223, Multiwavelength Investigations of Solar Activity, ed. A. V. Stepanov, E. E. Benevolenskaya & A. G. Kosovichev (Cambridge: Cambridge Univ. Press), 367
Neidig, F. 2004, BAAS, 36, 738
Neidig, D., et al. 1998, in ASP Conf. Ser., 140, Synoptic Solar Physics, ed. K. S. Balasubramaniam, Jack Harvey, & D. Rabin (San Francisco: ASP), 519
Okamoto, T. J., Nakai, H., Keiyama, A., Narukage, N., Ueno, S., Kitai, R., Kurokawa, H., Shibata, K. 2004, ApJ, 608, 1124
Pevtsov, A. A. 2000, ApJ, 531, 553
Scherrer, P. H., et al. 1995, Sol. Phys., 162, 129
Schmieder, B., Lin, Y., Heinzel, P., & Schwartz, P. 2004, Sol. Phys., 221, 297
Smith, S. F., & Harvey, K. L. 1971, in Physics of the Solar Corona, ed. C. M. Marcis (Dordrecht: Reidel), 156
Thompson, B. J., Plunkett, S. P., Gurman, J. B., Newmark, J. S., St. Cyr, O. C., & Michels, D. J. 1998, Geophys. Res. Lett., 25, 2465
Thompson, B. J., et al. 1999, ApJ, 517, L151
Uchida, Y. 1968, Sol. Phys., 4, 30
Vršnak, B., Warmuth, A., Brajša, R., & Hanslmeier, A. 2002, A&A, 394, 299
Warmuth, A., Mann, G., & Aurass, H. 2005, ApJ, 626, L121
Warmuth, A., Vršnak, B., Aurass, H., & Hanslmeier, A. 2001, ApJ, 560, L105
White, O. R., & Wilson, P. R. 1966, ApJ, 146, 250
Yashiro, S., Gopalswamy, N., Michalek, G., St. Cyr, O. C., Plunkett, S. P., Rich, N. B., & Howard, R. A. 2004, J. Geophys. Res. Space Phys., 109, 7105